Assessment of the Cycle-to-Cycle Noise Level of the Geosat Follow-On, TOPEX, and Poseidon Altimeters

N. TRAN

Raytheon ITSS and NASA Goddard Space Flight Center/Wallops Flight Facility, Wallops Island, Virginia

D. W. HANCOCK III AND G. S. HAYNE

NASA Goddard Space Flight Center/Wallops Flight Facility, Wallops Island, Virginia

D. W. LOCKWOOD

Raytheon ITSS and NASA Goddard Space Flight Center/Wallops Flight Facility, Wallops, Virginia

D. VANDEMARK

NASA Goddard Space Flight Center/Wallops Flight Facility, Wallops, Virginia

M. L. DRISCOLL AND R. V. SAILOR

TASC, Inc., Reading, Massachusetts

21 September 2001 and 1 April 2002

ABSTRACT

The Geodetic Satellite (Geosat) Follow-On (GFO), Ocean Topography Experiment (TOPEX), and Poseidon altimeter white-noise levels have been evaluated using a technique based on high-pass filtering of 1-Hz sea surface height time series. High-pass filtering removes the geoid and oceanography signals while revealing the random noise. This filtering technique is simpler to use than the repeat-track method, gives essentially the same results, and makes it easier to analyze much larger amounts of data to investigate subtle variations in noise levels. The new noise-level measurements provided here all show stable noise-process characteristics from cycle to cycle, with a linear dependence of the noise level upon significant wave height (SWH). The GFO altimeter noise level is estimated to be 2.5 cm for an SWH of 2 m. The Poseidon noise level is estimated at 2.0 cm for the same value of 2 m SWH. The TOPEX altimeter noise level is 1.8 cm when the dual-frequency ionospheric correction is included; when this noisy correction is not used, the level is reduced to 1.5 cm. Although the dual-frequency ionospheric correction provides an average improvement over the ''Doppler orbitography and radiopositioning integrated by satellite'' (DORIS) correction, high-frequency noise enters into the dual-frequency correction via noise from the Ku- and C-band ranges. Because the variations in ionospheric refraction are a relatively long wavelength global effect (with strong dependence on latitude), the dual-frequency ionospheric correction should be low-pass filtered before use, and this correction should not be included when estimating the high-frequency noise level of the altimeter.

1. Introduction

The Geodetic Satellite (Geosat) Follow-On (GFO) and the Ocean Topography Experiment (TOPEX)/Poseidon (T/P) missions are dedicated to the observation of the ocean surface topography from orbit using satellite-based nadir-pointing radar altimeters. The basic data are altimeter-derived sea surface heights (SSH) that are obtained by taking the difference of the satellite altitude (relative to a reference ellipsoid) as determined by precision orbit tracking and the altimeter range as determined by precise measurement of the round-trip

Corresponding author address: Dr. Ngan Tran, CLS/Space Oceanography Division, 8-10 rue Hermes, 31526 Ramonville St-Agne, France.
E-mail: tran@cls.fr

time of flight of the radar signal. The range estimate requires environmental corrections, for example, for atmospheric propagation delays and sea-state biases. Measurements of the range in 1-s averages are generally analyzed in applications of altimeter data.

An integral part of the analysis of altimeter datasets is a quantitative evaluation of altimeter instrument noise. This is necessary for monitoring improvements in measurement systems, for projecting future capabilities, and for properly analyzing the data in oceanographic and geodetic applications. The precision of satellite radar altimeter instruments has improved since the earlier programs [the *Geodynamics Experimental Ocean Satellite* (*GEOS-3*), Seasat, and Geosat], and continuous improvements in environmental corrections (orbits, ionospheric refraction, tides, etc.) have resulted in modern altimeters (e.g., TOPEX) having absolute errors of only a few centimeters.

The largest contributions to the measured sea surface topography come from 1) geoid undulations, 2) dynamic oceanography associated with geostrophic surface currents and eddies, 3) tides, 4) the sea surface response to atmospheric pressure loading, and 5) altimeter instrument noise; not included in this list are orbit errors, which are very long in wavelength and relatively small in amplitude and which may be ignored for the purpose of this discussion. The elevation variability of the geoid signal is on the order of meters to tens of meters; the oceanographic signals are from a few centimeters to no more than 2 m; and tides in the open ocean are generally less than 1 m but can be predicted by numerical models to better than a few centimeters. The atmospheric loading or ''inverse barometer'' effect is a few centimeters, and the instrument noise is also at the few-centimeter level. One additional, but small, effect comes from ocean waves and swell. Although very obvious to mariners, waves are not a major factor in the measured sea surface topography, because each altimeter pulse illuminates a circular area on the ocean that is several kilometers in diameter, so the local waves are approximately averaged out. Actually, the averaging out is not perfect, and there is an ''electromagnetic bias'' correction proportional to significant wave height (SWH) and wind speed that should be made for the most precise uses of altimeter data (e.g., Gaspar et al. 1994).

The original analyses of satellite altimeter noise were developed in the context of geodesy, and ''noise'' was defined as any effect in the data other than the geoid signal. Noise was studied by comparing the repeatability of the data observed along colinear or repeat tracks. By differencing the data series along two repeat tracks (having a cross-track offset of no more than 1 km), the time-invariant geoid signal cancels out and a time series of random noise remains. Spectral analysis of the difference time series reveals two main components of the noise: 1) a ''colored'' noise process behaving approximately like a first-order Markov random process (this is attributable to oceanography) and 2) a lower-powered additive contribution that appears as a ''white-noise floor,'' visible as the noise spectra flatten out at high frequency (Brammer and Sailor 1980; LeSchack and Sailor 1988). The white-noise component was attributed to electronic noise in the altimeter instrument, and, indeed, the on-orbit results are generally consistent with laboratory measurements of instrument noise made before launch.

However, as this paper shows, a portion of the white-noise component can be attributed to random scattering effects from ocean waves, since the white-noise level is found to be proportional to the SWH. The repeat-track method of studying noise in altimeter data requires that repeat tracks be matched up and aligned, that environmental corrections (e.g., tides) be applied independently to each track, and that power spectra be computed from the difference segments. This is straightforward but was not easily automated to process large amounts of data. Consequently, the early studies did not apply this method to very many repeat-track pairs and did not investigate in much detail the variability in noise that might occur as a function of aging of the spacecraft or that might be due to environmental factors such as SWH. Nevertheless, the white-noise level for each altimeter was found to be fairly consistent, and the average values obtained for different altimeters are a good measure of the relative quality of those instruments. For example, *GEOS-3*, launched in 1975, had a white-noise level of about 23 cm. For Seasat in 1978 the result is 5 cm, and for Geosat in 1985 it was 3 cm (Sailor and LeSchack 1987; Sailor and Driscoll 1992). Le Traon et al. (1994) analyzed TOPEX and Poseidon spectra and estimated that the Poseidon repeat-track noise level is about 3 cm and the TOPEX repeat-track noise level is about 1.8 cm, calculated as rms. All of these numbers have been determined without consideration of the SWH. They all represent the integrated white-noise power in the frequency band from -0.5 to $+0.5$ Hz (the folding frequencies for data sampled at 1 Hz), so these noise values correspond to a 1-s average. Sailor (1993) defines the signal processing and spectral analysis techniques in detail and gives examples that confirm the validity of the noise-modeling approach that involves repeat tracks.

More recently, investigations by Driscoll and Sailor (2001) have shown that, since white noise dominates the GFO altimeter SSH time series at the shortest wavelengths, a noise measurement algorithm that works by high-pass filtering 1-Hz data to estimate the white-noise level is a good and simple alternative method. They have demonstrated the robust nature of this simplified, single-track analysis approach that avoids the need 1) to obtain and align repeat tracks, 2) to apply environmental corrections, and 3) to compute power spectra of difference time series. They used 52 GFO track segments for their study, and the amount of data along these segments varied from approximately 180 to 830 samples. In addition to developing a single-track filtering method that

gives the same results as the repeat-track method, they also showed that the noise level is sensitive to SWH, as expected; the noise level increases linearly with increasing SWH. The GFO altimeter was designed to have an rms white-noise level, based on 1-s height averages, of less than 3.5 cm for significant wave heights of less than 2 m. The results of Driscoll and Sailor's (2001) analysis show that the GFO noise level is better than 2.7 cm for SWH of less than 2 m, demonstrating that the GFO altimeter meets its design specification.

Several issues that have not been addressed in past analyses of radar altimeter performance will be discussed in the following. We first extended this high-pass filtering method from a segment evaluation to a cycle evaluation for GFO data. This method is simple to implement as an automatic process and will serve the purpose of providing a cycle-by-cycle instrument characterization. We will then apply the method to quantify the white-noise level of the TOPEX and Poseidon altimeter data as a function of the SWH for comparison. In the TOPEX case, we compare the result with the operational dual-frequency range noise estimation. This latter technique has been developed specifically for dual-frequency altimeters such as TOPEX and is not applicable to single-frequency altimeters such as GFO and Poseidon. We will also discuss the influence of the atmospheric corrections to the range in the TOPEX noise-level estimations.

Datasets and the processing routines are described in the next section. Estimates of the GFO noise level are presented in the section 3. Sections 4 and 5 concern, respectively, TOPEX and Poseidon altimeter noise analysis. The last section discusses the main results of this study.

2. Datasets and processing

a. Geosat Follow-On

The GFO, a U.S. Navy project, is one of a series of radar altimeter satellites. GFO was launched on 10 February 1998. Its primary instrument is a nadir-pointing radar altimeter operating at a frequency of 13.5 GHz. Data presented here are based on the ''navy geophysical data records'' files, were collected from yearday 352 (17 December) of 2000 to yearday 155 (4 June) of 2001, and represent 10 repeat cycles of 17 days: cycle 1 through cycle 10. This study is based on the 1-Hz measurements of SSH with environmental corrections: wet and dry tropospheric corrections, ionosphere correction, and sea-state bias, along with inverse barometer and tide effects. In comparison with TOPEX/Poseidon SSH, there are more corrections applied to the GFO measurements, but the additional inverse barometer and tide effects contribution will not affect the high-frequency noise-level estimates since they come from models.

To eliminate anomalous data, rather stringent editing is applied through use of the GFO quality words I and II, which report on the altimeter measurement conditions such as height, automatic gain control, SWH, backscatter, range rate, off-nadir errors, fine track, ocean/land states, and rain conditions. Data are also discarded when they lie outside the latitude range 60°S–60°N and when the radar cross section σ_0 and SWH are, respectively, above 16 dB and 10 m.

b. TOPEX/Poseidon

The TOPEX and Poseidon altimeters fly on the T/P satellite launched 10 August 1992. This mission is jointly conducted by the U.S. and French space agencies. The altimeters are, respectively, designed by the National Aeronautics and Space Administration (NASA) and by the Centre National d'Etudes Spatiales (CNES). TOPEX is a dual-frequency Ku-/C-band radar altimeter operating at 13.6 (Ku band) and 5.3 (C band) GHz simultaneously, and Poseidon is a single-frequency altimeter operating at 13.65 GHz. The TOPEX C-band capability is principally for improving estimates of the ionospheric correction. TOPEX is the primary sensor for the T/P mission, and Poseidon is an experimental instrument used to validate the technology of a low-power, lightweight altimeter for future Earth-observing missions. It shares the antenna used by TOPEX; thus, only one altimeter operates at any given time. Poseidon operates approximately 10% of the time.

The datasets are based on the ''merged geophysical data records'' files, which are produced operationally, for a cycle of 10 days, by the Archiving, Validation, and Interpretation of Satellite Data in Oceanography (AVISO) center. These files contain data from both the TOPEX dual-frequency and the Poseidon solid-state altimeter. For TOPEX the advantage is to have two different ionospheric corrections available as reviewed in the following. The TOPEX files, for this study, cover a period of eight cycles (cycles 304–312, except 307), from yearday 349 (14 December) of 2000 to yearday 72 (13 March) of 2001. These cycles were chosen because they sampled the ocean surface during the same period of time as the first five cycles of GFO. The T/P files for the entire period covered by our chosen GFO cycles were not all available at the time of this study. Because Poseidon operates about 10% of the time, our dataset, over this period, contains only one cycle, cycle 307 from yearday 13 (13 January) to yearday 23 (23 January) of 2001. We added five more Poseidon cycles acquired earlier, for assessment of the stability of the noise-level estimation with time (cycles 243 and 266 in 1999, and cycles 278, 289, and 299 in 2000).

The measurements used are 1-s averages. The SSH measurements are obtained using either the NASA orbit or the CNES orbit, depending on which altimeter is analyzed at the time. Note that, since the two orbits agree to within a few centimeters (Morris and Gill 1994), either of these orbits could have been used for both altimeters. The standard corrections (wet and dry

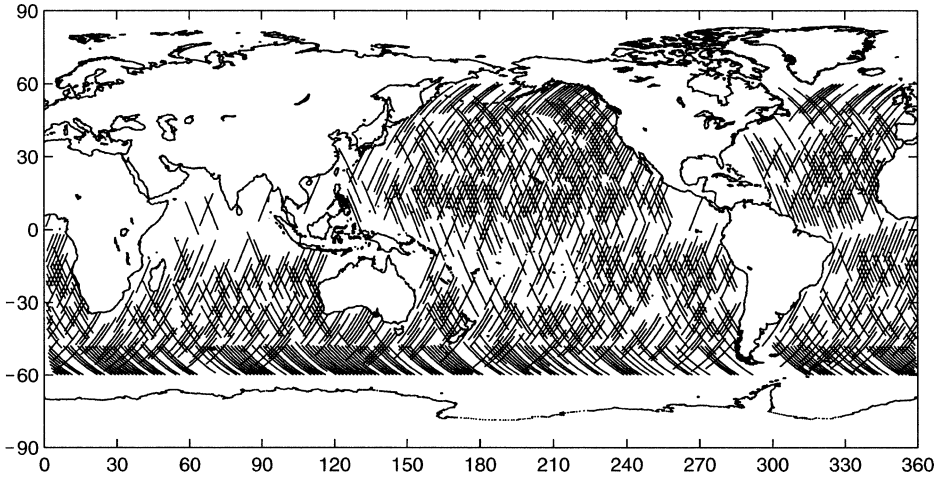

FIG. 1. Spatial distribution of the 5-min track segments used to assess the noise-level estimates for cycle 7 of GFO.

tropospheric corrections, ionosphere correction, and sea-state bias) applied to the range measurements to compute the SSH come from the same sources for both TOPEX and Poseidon, except for the ionospheric correction. For TOPEX, the two-frequency measurements are used to compute the effect of ionospheric free electrons in the satellite range measurements. Since Poseidon uses a single frequency, an external correction for the ionosphere must be applied. This latter comes from the ''Doppler orbitography and radiopositioning integrated by satellite'' (DORIS) measurements. DORIS's main purpose is to constrain the computed position of the satellite, in conjunction with a large number of ground stations. It also measures in two carrier frequencies (0.4 and 2 GHz) to correct for ionospheric delays to its signal, but the paths between the satellite and DORIS ground stations are usually slanted off vertical, whereas the altimeter's path is vertical. The DORIS slant-path delays are used together with an ionospheric model (the Bent model of R. B. Bent) to estimate the vertical-path delay.

For this study, the TOPEX and Poseidon altimeter data are also limited in space between latitudes 60°S and 60°N, as applied for GFO data. In addition to the data flags (Alt_Bad, Geo_Bad, and telemetry flags), all cases with satellite platform attitude angle larger than 0.12° are eliminated. Also discarded are measurements taken when σ_0 and SWH are, respectively, above 16 dB and 10 m. Note that TOPEX and Poseidon have good attitude angle corrections up to 0.45° and 0.30°, respectively. The lower limit set here comes from the editing process routinely used at Wallops Flight Facility, in Virginia, to monitor TOPEX altimeter measurement quality, as explained in the following, and allows us to compare the results from the high-pass filtering process with the ones from the actual Wallops operational process, presented in section 4b, on the same filtered data.

Last, we have been investigating a phenomenon referred to as ''σ_0 blooms,'' and a paper reporting the results is in preparation. A σ_0 bloom is characterized by abnormally high values of the ocean surface radar backscattering cross section. They are seen in all space-

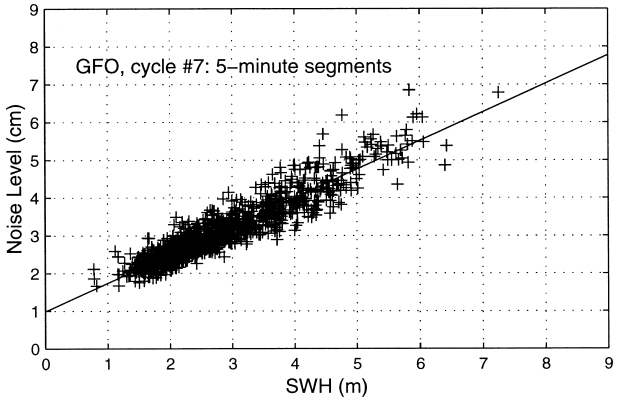

FIG. 2. GFO rms white-noise-level estimates with respect to SWH based on 5-min track segments of cycle 7 of GFO.

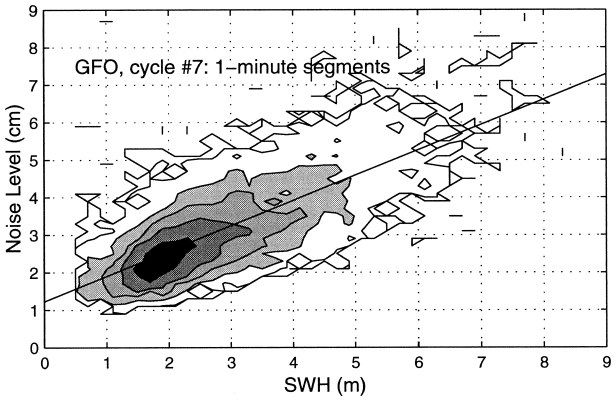

FIG. 3. GFO rms white-noise-level estimates with respect to SWH based on 1-min track segments of cycle 7.

TABLE 1. Statistical indicators for GFO based on 5- and 1-min track segments. The values represent averages over the 10 cycles analyzed.

	Ku SWH		Noise level (NL)		NL vs Ku SWH		
GFO	Mean (m)	Std dev (m)	Mean (cm)	Std dev (cm)	Slope	Intercept	NL at 2-m SWH
5-min	2.745	1.085	3.077	0.883	0.754 ± 0.010	1.006	2.515
1-min	2.580	1.225	2.978	1.154	0.688 ± 0.006	1.202	2.579

borne radar altimeter data, not just TOPEX, can persist for tens of seconds, and contaminate some several percent of all the over-ocean data.

In these regions of anomalous Ku-band σ_0 values (higher than 13–13.5 dB) the altimeter mean return waveform shape departs from the expected shape, which is based on a purely incoherent scattering model. The off-nadir angle obtained from the shape of the return waveform becomes unreliable and is set to a large value that signals an attitude estimation error. Thus the waveform-estimated attitude will vary significantly even though the actual spacecraft attitude angle is almost constant. A data-editing criterion of 0.12° for the waveform-based attitude estimate is then used, rejecting data outside this value. Because of the performance history of the spacecraft attitude control system (generally maintaining an off-nadir attitude of 0.10° or less), effectively no valid data will be rejected by this 0.12° criterion, but some σ_0-bloom-contaminated data may be removed from the dataset to ensure data quality.

c. Data processing

The application of the editing procedure leads to gaps in the SSH time series. To retain as many segments as possible, short 2–5-s gaps are filled using linear interpolation. This interpolation, done on a very small percentage of the data, does not affect the results. The rms noise levels are then computed using the high-pass-filter method. In this method, the time series are first filtered using a fifth-order Butterworth high-pass filter with a cutoff frequency of 0.30 Hz to isolate the high-frequency instrument noise and remove the lower-frequency geophysical signals. The output of the filter is high-pass-filtered white noise that has an rms proportional to the rms of the white-noise floor in the original data. The filter output is next edited to remove filter startup transients, spikes, and other atypical data points. The rms of this output time series is then computed and scaled to give the rms white-noise level of the 1-Hz altimeter time series. The scale factor for our particular filter is 1.574. Scale factors for other filters can be determined by computing the square root of the reciprocal of the integrated power gain function for the particular filter. This is equivalent to computing the ratio of the rms values of an input time series (white noise) and the high-pass-filtered output.

The method was applied to GFO data on two different track segment sizes, 290–310 samples (~5 min) and 50–70 samples (~1 min), to evaluate the accuracy of the estimations. For both TOPEX and Poseidon, only the results based on 5-min segments are reported in this paper, with an exception made for TOPEX when we do the comparison with the Wallops noise-level estimation algorithm, which works on a 1-min time window.

3. GFO noise level

Figure 1 shows the spatial distribution of the 5-min track segments used to assess the noise level for cycle 7 of GFO. The average number of segments per cycle is approximately 1026 for the cycles used in this study. Note that, because of the editing process and the segment length choice, some regions of the global ocean, such as the northern Indian Ocean, the Mediterranean Sea, or the western part of the North Atlantic Ocean, are less represented than other regions, although most of the global ocean is covered. Note also that, because of the retrograde orbit of GFO, the segmentation of the time series, and the latitude restriction for the coverage, there are fewer descending than ascending track segments taken into account in the Southern Ocean below 50°S. We observed the opposite above 50°N. At the end of the passes, ascending or descending, the amount of remaining ''valid'' data is not sufficient to provide a 5-min segment. We observed that when the track segment length is reduced to a 1-min interval, the average number of segments increases to about 9400, and their spatial distribution provides better coverage of small areas.

Figures 2 and 3 show the high-pass-filtering estimates of the GFO rms white-noise level with respect to the SWH, based, respectively, on the 5- and 1-min track segments of cycle 7 of GFO. SWH-averaged values along the track segments vary from 0.5 to 7 m, providing a good sampling of calm to rough sea surface conditions. Values of rms noise level are mostly between 2 and 6 cm for the 5-min segments and between 1 and 7 cm for the 1-min ones. In this latter plot, the data are shown by density contours to better display where most of the data are. The two-dimensional histogram exhibits a peak around 2-m SWH and 2.5-cm noise level. The decrease of the segment size from 5 to 1 min increases the representation of lower (<1.25 m) and higher (>5 m) SWH values, leading to a larger variability of the noise-level estimates with respect to SWH. The noise level is sensitive to SWH, with larger noise values associated with

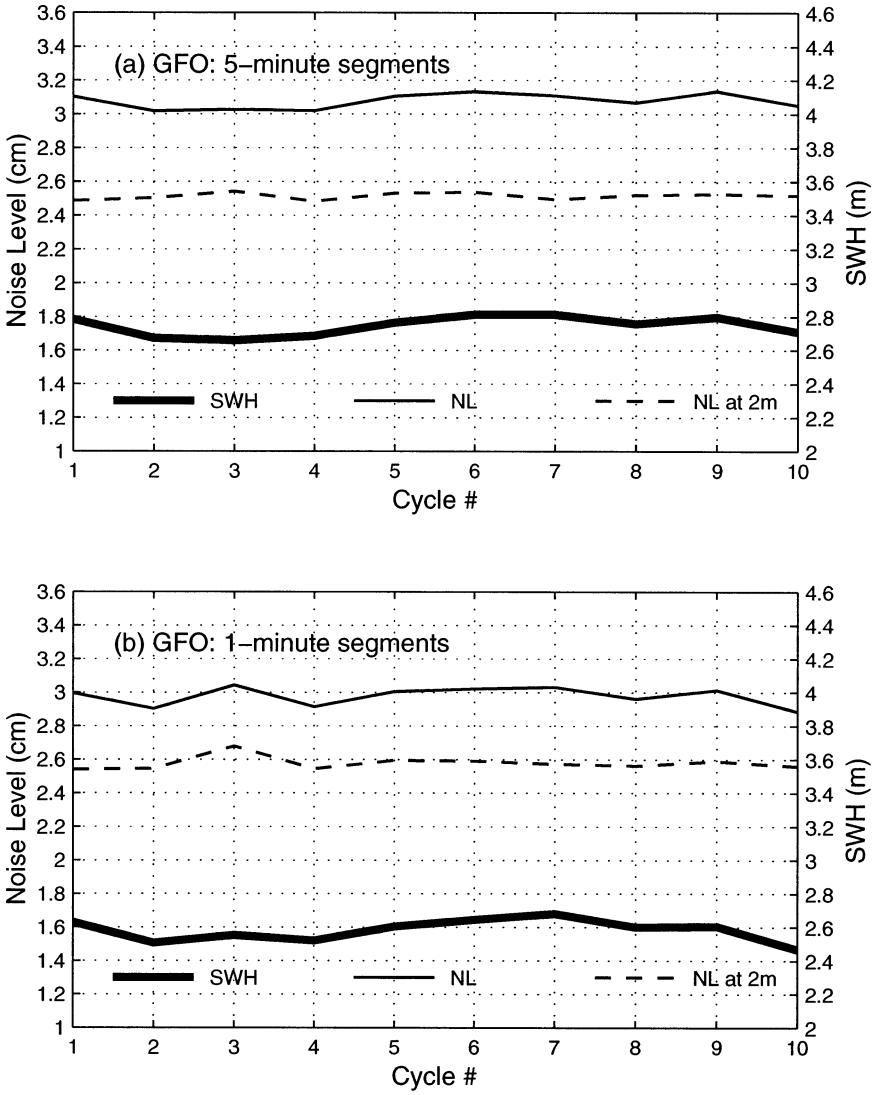

FIG. 4. Variation of the average value of the noise level (NL) and SWH for each GFO cycle, along with the value of the noise level at 2-m SWH, determined from the linear fit, as a function of the cycle number: (a) results for the 5-min segments and (b) results for the 1-min segments.

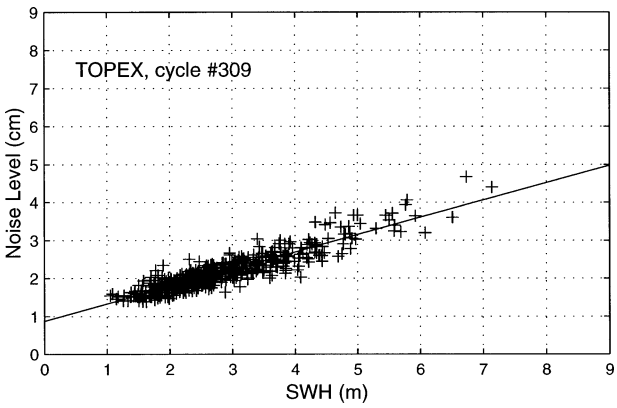

FIG. 5. TOPEX rms white-noise-level estimates with respect to SWH based on 5-min track segments of cycle 309.

larger SWH. The straight line in Figs. 2 and 3 represents a linear least squares fit. As shown in Driscoll and Sailor's (2001) results, the noise level increases linearly with increasing SWH.

Table 1 summarizes the averaged statistical indicators from such plots over the full set of 10 GFO cycles studied, and Fig. 4 displays, as a function of the cycle number, the average value of the noise level and SWH for each cycle, along with the value of the noise level at 2-m SWH, determined from the linear fit. The small variations in the averaged noise level follow those in the averaged SWH. The noise level at 2-m SWH is a stable indicator that can be used to characterize the altimeter noise level for both track segment sizes. Table 1 shows a 6% decrease of the mean of the Ku-band SWH distribution when the segment size is reduced.

TABLE 2. Statistical indicators for TOPEX based on 5-min segments. The values represent averages over the eight cycles analyzed (w/o: without; iono: ionospheric correction).

	Ku SWH		Noise level (NL)		NL vs Ku SWH		
TOPEX	Mean (m)	Std dev (m)	Mean (cm)	Std dev (cm)	Slope	Intercept	NL at 2-m SWH
With iono	2.831	1.015	2.177	0.524	0.466 ± 0.010	0.855	1.788
W/o iono	2.831	1.015	1.888	0.487	0.432 ± 0.010	0.662	1.527

The mean of the rms noise level remains at a stable value of about 3.0–3.1 cm. The two noise-level estimates at 2-m SWH are equivalent, with a value of 2.5–2.6 cm. The slope of the linear fit between the rms noise level and the Ku-band SWH shows a decrease of about 9%. This is due to the fact that the *x*-axis regressor is much more ''smeared'' with the 5-min average, so the slope heads lower because more low wave heights leak into the SWH average. The errors on the slopes and on the intercepts are, respectively, about 0.01 and 0.03.

The results obtained with the 1-min track segments do not differ much from the results obtained with the 5-min segments. Since the results from the 5-min segments exhibit a smaller variability in the noise level estimate with respect to SWH, they will be reported for both TOPEX and Poseidon in the next two sections and will be used to compare the three altimeter performances. The advantage of this noise estimation is that it can be applied to single-frequency altimeter data, such as from GFO or Poseidon, as well as to dual-frequency altimeter data, such as from TOPEX. This method allows comparison of the quality of different altimeters in a straightforward manner without having to work with repeat tracks.

4. TOPEX noise level

Figure 5 shows the high-pass-filtering estimates of TOPEX rms white-noise level with respect to SWH for the 5-min track segments of cycle 309 of TOPEX. The average number of segments per cycle is about 510. Values of rms noise level vary mostly between 1 and 3 cm, and this interval of variability is lower for TOPEX than for GFO (Fig. 2). Table 2 presents the averaged statistical indicators computed over the eight TOPEX cycles studied, and Fig. 6a displays the average value of the noise level and SWH for each cycle along with the value of the noise level at 2-m SWH as a function of the cycle number. The gap at cycle 307 is due to the operation of the Poseidon altimeter. The errors on the slopes and on the intercepts are, respectively, about 0.01 and 0.04. The same comment as for GFO can be made; the noise level at 2-m SWH is a stable indicator, with an average value of about 1.8 cm over the eight TOPEX cycles. The mean value of the rms noise-level distribution for each cycle is somewhat higher, with a value of about 2.2 cm. Note that comparison of the slope of the linear fit between the noise level and SWH exhibits a lower value for TOPEX than for GFO. This is discussed in more detail in section 6.

a. Dual-frequency ionosphere correction effect

In the TOPEX case, there are additional considerations when quantifying our results. The high-pass filter is applied to the SSH values that are computed from the satellite altitude and the altimeter range with atmospheric propagation corrections. We note that estimating the white-noise level based on the SSH measurements could be viewed as an estimation of the white-noise level on the altimeter range itself if there were no high-frequency content in the range corrections applied. However, as recalled by Stammer and Wunsch (1994), Callahan (1992) recommended that the raw ionospheric corrections should be averaged over a 21-s moving window to eliminate high-frequency noise. This noise comes from the TOPEX algorithm used to compute the ionospheric correction. The ionosphere directly affects the altimeter measurement by increasing the electromagnetic-path delay to the surface in proportion to the total electron content along the path; that increase would translate as errors in sea level. Since the delay is inversely proportional to frequency squared, the TOPEX dual-frequency altimeter measures this delay at two different frequencies, allowing the error to be corrected. By employing range measurements at a different frequency to obtain an ionosphere correction, one propagates the errors from both individual ranges into this correction. Thus the ionosphere correction, contaminated with the altimeter range measurement noise, has high-frequency components that raise the noise level estimated by high-pass filtering the 1-Hz TOPEX SSH data.

Table 2 also presents the averaged statistical indicators estimated from the SSH measurements time series after removing the ionospheric corrections. Figure 6b shows the revised variations with respect to the cycle number, clearly indicating a decrease of the noise level. The mean value of the rms noise-level distribution for each cycle is reduced to about 1.8–2.0 cm, which represents a decrease of 13.3%. The noise level at 2-m SWH decreases by 14.6% and becomes about 1.5 cm. The slope of the linear fit decreased by 7.3%, which is explained by the fact that both the range noise, which is correlated with SWH, and the ionospheric electron content exhibit a latitudinal dependence.

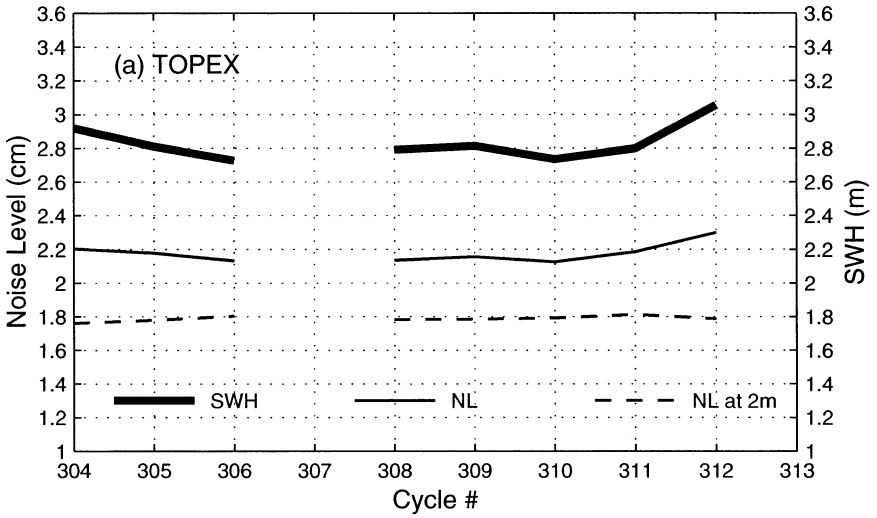

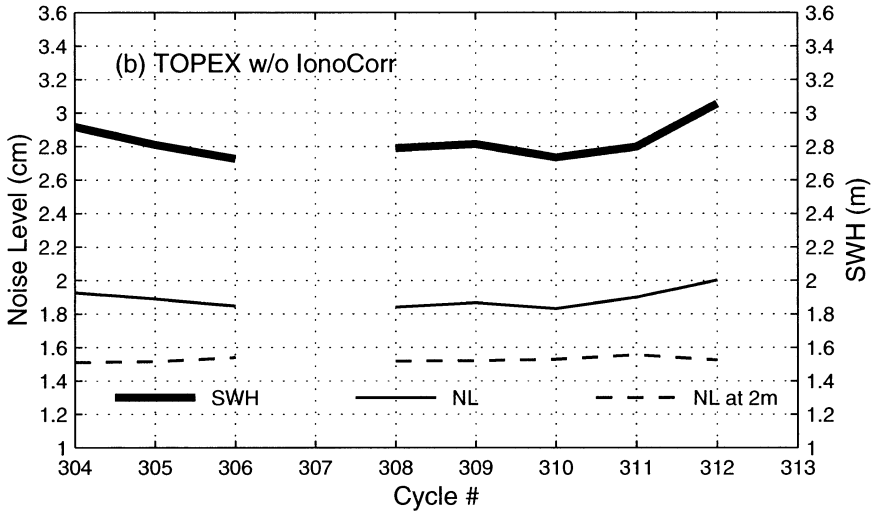

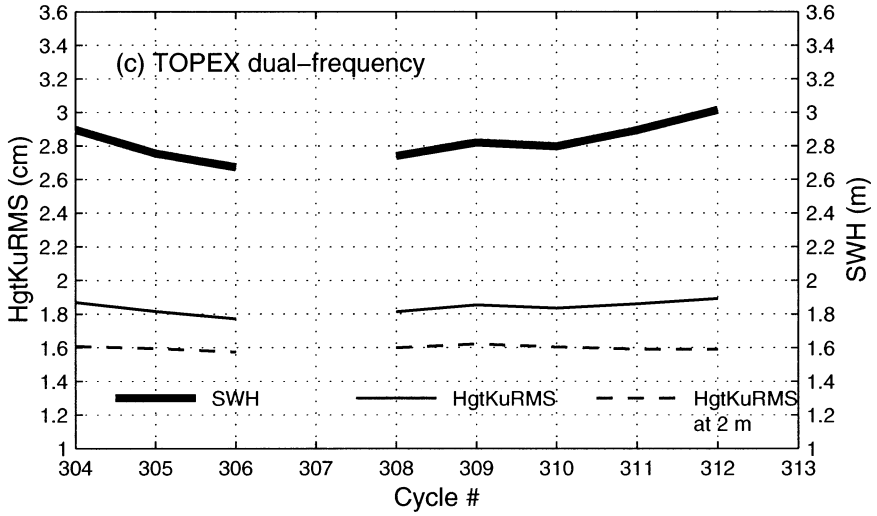

TABLE 3. Statistical indicators for TOPEX based on 1-min track segments of the 1) combined-frequency, 2) Ku-band, and 3) C-band ranges by the high-pass-filtering process, and 4) results by the Wallops operational process. The values represent averages over the eight cycles analyzed.

	Ku SWH		Noise level (NL)		NL vs Ku SWH		
TOPEX	Mean (m)	Std dev (m)	Mean (cm)	Std dev (cm)	Slope	Intercept	NL at 2-m SWH
Combined	2.793	1.216	1.913	0.704	0.417 ± 0.006	0.749	1.582
Ku-band	2.793	1.216	1.764	0.675	0.397 ± 0.005	0.653	1.448
C-band	2.793	1.216	3.357	0.988	0.558 ± 0.008	1.800	2.916
Wallops	2.824	1.139	1.838	0.421	0.292 ± 0.006	1.014	1.597

The total electron content of the ionosphere varies depending upon the time of day, solar conditions, geographic location, and satellite altitude (Callahan 1984). Total electron content is largest when the sun is overhead and at all local times near $\pm 15^\circ$ geomagnetic latitude. These variations are generally of long wavelength, however. The ionosphere correction is then, on average, correlated with ocean SWH through its latitudinal dependence (Imel 1994). The ionospheric electron content and SWH show a 15% correlation (Zlotnicki 1994). So, the relationship between the noise-level estimates and SWH changes when we remove the ionosphere correction, leading to the observed change in the slope of the linear fit.

We next used the DORIS ionosphere correction provided by CNES as an independent source to verify that the high-frequency component in the dual-frequency ionospheric correction comes from the range measurement noise. The advantage of the DORIS ionosphere correction over the NASA one is that it is independent of the altimeter range measurement. Its disadvantage is that, in general, it is less accurate because the ionosphere sampled by the DORIS system is not the ionosphere sampled by the altimeter. Ionospheric electron content from DORIS, which involves a space–time interpolation among slant paths between the satellite and fixed ground stations, should have larger errors near the equator, where the large electron content variability may not be sampled rapidly enough or closely enough (Zlotnicki 1994).

The replacement of the dual-frequency ionosphere correction by the DORIS one leads to the result that the rms noise level stays low, as it was when we simply removed the TOPEX ionosphere correction from the SSH before applying the high-pass-filtering process. Thus, the TOPEX dual-frequency ionospheric correction clearly introduces additional high-frequency noise leading to an increase of the rms noise level estimated by high-pass filtering of the SSH time series. So, for the purpose of characterizing the noise level related to the altimeter instrument, it is better to first low-pass filter, or just not use, any corrections that are not long-wavelength in nature. Note that for GFO data the ionospheric correction comes from ionosphere models and should not affect the noise-level estimation.

The impact of the three other corrections in TOPEX SSH, the dry and wet tropospheric corrections, and the sea-state bias, has also been analyzed. The sea-state bias, similar to the dual-frequency ionospheric correction, has a high-frequency component. This is due to the same reason; both the dual-frequency ionosphere correction and the sea-state bias are obtained using empirical models derived from analyses of altimeter data itself. The sea-state bias is computed from SWH and the wind speed derived from the radar cross section (Gaspar et al. 1994). This correction contributes about 0.04 cm to the mean value of the rms noise level. The two atmospheric corrections, the dry and wet tropospheric corrections, are both long-wavelength effects. The dry tropospheric correction is determined from the European Centre for Medium-Range Weather Forecasts model surface pressure values, and the wet tropospheric correction comes from the TOPEX microwave radiometer. Even if the wet tropospheric correction comes from measurement, removing either one of the two tropospheric corrections from the SSH measurements does not change the noise-level estimates. Among the corrections applied to the range, the dual-frequency ionosphere correction thus has the largest contribution to the TOPEX altimeter noise level.

b. Comparison with the Wallops operational estimation

The operational technique we have been using to estimate the performance of the TOPEX Ku-band altimeter is a 1-min-averaged rms based on calculating the rms of one-per-frame Ku-minus-C height differences.

←

FIG. 6. Variation of the average value of NL and SWH for each TOPEX cycle, based on 5-min segments, along with the value of NL at 2-m SWH, determined from the linear fit, as a function of the cycle number, computed (a) from SSH, (b) from SSH after removing the TOPEX ionospheric correction, and (c) by the dual-frequency method. [Height rms for the Ku band (Hgt KuRMS) is the Wallops operational noise-level estimation.]

TABLE 4. Altimeter performance for TOPEX combined-frequency, Ku-band, and C-band ranges at 2-, 4-, and 6-m SWH, based on the 1-min segments of SSH time series computed with the uncorrected range values.

	Ku SWH (m)		
Altimeter 1-min	2	4	6
Combined	1.58	2.41	3.25
Ku-band	1.45	2.24	3.04
C-band	2.92	4.03	5.15

The height rms for the Ku band is then determined by scaling the Ku-minus-C height difference rms by a factor that depends on the Ku:C noise ratio. In most of the TOPEX data, the C-band range standard deviation is expected to be between 1 and 2 times the Ku-band range standard deviation (because of a poorer signal-to-noise ratio and less pulse-to-pulse averaging); a fixed ratio of 1.6 has been used. This method takes the effects of geoid variation out of the calculation, since both frequencies follow the same geoid tracking. This method has been developed specifically for a dual-frequency altimeter such as TOPEX and cannot be used for a single-frequency altimeter.

To compare with this operational estimation of the 1-min-averaged Ku-band range noise, we compute the noise-level estimates with the high-pass-filtering process on the 1-min track segments of the ''uncorrected'' SSH time series, that is, computed with the uncorrected range (without the ionospheric correction, tropospheric corrections, and the sea-state bias). Noise level estimates based on the combined dual-frequency range data along with, respectively, the Ku- and C-band range data are presented in Table 3. As expected, the C-band noise (average value of ~3.4 cm) is higher than the Ku-band noise (average value of ~1.8 cm), and the combined noise (average value of 1.9 cm) lies between the two but is closer to the Ku-band noise. The combined range is computed as $R = 1.18R_{\mathrm{Ku}} - 0.18R_C$ (Chelton et al. 2001). It is apparent that the combined range weights the Ku-band range estimate about 6.6 times as much as the C-band range. The higher C-band measurement errors are of secondary concern in the combined range noise since they are reduced by the multiplicative factor 0.18. Table 4 summarizes the TOPEX altimeter performance, listing the rms noise level of the combined-frequency, Ku-band, and C-band altimeter at respectively 2-, 4-, and 6-m SWH. The ratio between C and Ku band varies between 1.7 and 2.0 with respect to SWH.

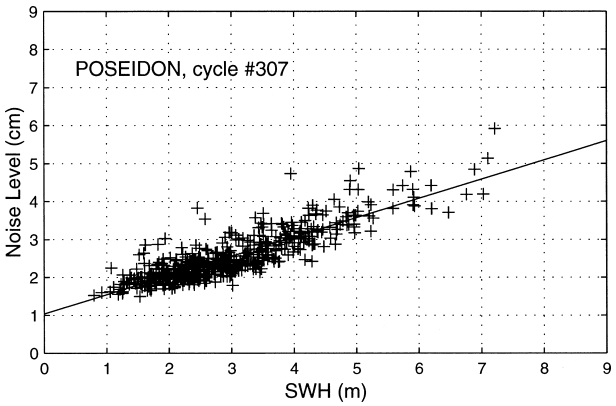

FIG. 7. Poseidon rms white-noise-level estimates with respect to SWH based on 5-min track segments of cycle 307.

This alternate Ku-band range noise estimation also displays a linear trend with respect to SWH. The averaged statistical indicators computed from this method (referred to as Wallops) are included in Table 3. All results in this table are derived from about 5400 rms noise estimates. The mean value of the Wallops Ku-band range noise level and the value at 2-m SWH from the linear fit with respect to the cycle number are shown in Fig. 6c. Both variations are stable with time. The noise level computed directly from the 1-min Ku-band range exhibits higher values by 4% for the mean and by 10% for the noise level at 2-m SWH than the ones obtained using the high-pass-filtering method applied to 1-min track segments and using Ku-band range. This is related to the fact that the operational algorithm used a fixed value for the ratio between the C-band and the Ku-band noise, whereas this ratio changes with SWH (as seen in Table 4). Although the two linear fits are different, the mean value of both distributions and the noise-level estimates at 2-m SWH are sufficiently close to conclude with confidence that these methods are equivalent.

5. Poseidon noise level

Figure 7 shows the high-pass-filtering estimates of the Poseidon rms white-noise level with respect to SWH based on the 5-min track segments of cycle 307 of Poseidon. Table 5 presents the averaged statistical indicators computed over the six Poseidon cycles studied. The errors on the slopes and on the intercepts are, respectively, about 0.01 and 0.05. Figure 8 displays the average value of the noise level and SWH for each cycle

TABLE 5. Statistical indicators for Poseidon based on 5-min track segments. The values represent averaged over the six cycles analyzed.

	Ku SWH		Noise level (NL)		NL vs Ku SWH		
Poseidon	Mean (m)	Std dev (m)	Mean (cm)	Std dev (cm)	Slope	Intercept	NL at 2-m SWH
5-min	2.977	1.139	2.543	0.695	0.519 ± 0.013	1.000	2.036

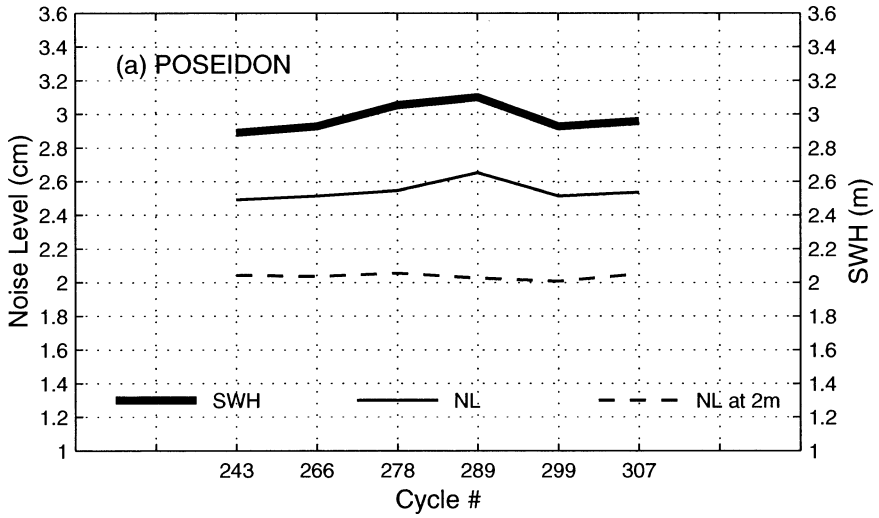

FIG. 8. Variation of the average value of NL and SWH for each Poseidon cycle (note the time discontinuities), based on 5-min segments, along with the value of NL at 2-m SWH, determined from the linear fit, as a function of the cycle number.

along with the value of the noise level at 2-m SWH as a function of the cycle number. There are about 600 five-minute track segments for each cycle. Note the very stable value of the rms noise level at 2-m SWH over time: it is about 2.0 cm, and the averaged value for a cycle is about 2.5 cm. This latter is slightly lower than the estimate reported by Le Traon et al. (1994), who found that the Poseidon repeat-track noise level is about 3 cm.

The high-pass-filtering process will be applied to the upcoming data of *Jason-1*, the follow-on to the highly successful TOPEX/Poseidon mission; *Jason-1* was successfully launched on 7 December 2001 and carries the CNES Poseidon-2 altimeter (Ku and C band).

6. Discussion and conclusions

Our analysis quantifies the performance of GFO, TOPEX, and Poseidon altimeters by evaluating the rms white-noise level as a function of SWH. Table 6 summarizes the altimeter performance for the three altimeters based on the 5-min segments of SSH time series, listing the rms noise level of each altimeter at, respectively 2-, 4-, and 6-m SWH. This comparison uses the rms noise-level estimates of TOPEX based on SSH measurements without the ionospheric correction because, as discussed earlier in section 4a, the TOPEX dual-frequency ionospheric correction introduces an additional high-frequency noise to the white-noise floor of the instrument, whereas for the single-frequency GFO and Poseidon this does not occur.

TABLE 6. Altimeter performance for GFO, TOPEX, and Poseidon at 2-, 4-, and 6-m SWH, based on the 5-min segments of SSH time series, except for TOPEX, for which we removed the ionospheric correction (w/o iono) in the SSH measurements.

	Ku SWH (m)		
Altimeter 5-min	2	4	6
GFO	2.51	4.02	5.53
TOPEX (w/o iono)	1.53	2.39	3.25
Poseidon	2.04	3.07	4.11

The rms noise level of TOPEX is the lowest at each SWH with a value of about 1.5 cm at 2-m SWH. Poseidon altimeter noise is higher, with a value of about 2.0 cm, and GFO altimeter noise is the highest, with 2.5 cm for the same SWH of 2 m.

Our results (Tables 2 and 6) show good agreement at 2-m SWH with a previous TOPEX/Poseidon altimeter performance evaluation that has been reported by Fu et al. (1994). They displayed the instrument noise at 1-Hz data rate as a function of SWH for both TOPEX and Poseidon. Their estimation of altimeter noise shows value of 1.7 cm at 2-m SWH for TOPEX, and Poseidon altimeter noise displays a higher noise level of 2.0 cm at 2-m SWH. Discrepancies with this earlier altimeter performance assessment are observed at higher SWH values and in the functional relationship linking the noise level to SWH. Fu et al. used a quadratic least squares fit, whereas a simple linear fit is used here and apparently captures the relationship.

As seen and expected, the different altimeters have different slopes of noise with SWH, a difference that can also be observed in the TOPEX altimeter between the two-frequency channels. This is related to the pulse repetition frequency (PRF) of the transmitted waveform, which is a critical performance driver, as discussed in Marth et al. (1993). This latter paper addressed in detail the impact of thermal receiver noise and ocean surface backscatter speckle noise on the height measurement. It pointed out that the speckle noise contributes the most in the height measurement uncertainties. This speckle

results from the fact that the fields scattered back to the altimeter from the ocean surface are the coherent sum of backscatter from many independently phased facets. The sea surface roughness shapes the leading edge of the waveform such that calm and rough seas generate steep and slanting leading edges, respectively. The sharply rising leading edge is the basis for the precise height estimation but also results in degraded measurement precision with increasing wave height.

The noisiness of each individual waveform can be reduced by averaging the waveforms for a Gaussian wave-height distribution. If the individual waveforms in the average are statistically independent (which depends on the pulse repetition rate and the satellite ground-track velocity), the noise decreases as the square root of the number of waveforms in the average (Chelton et al. 2001).

To minimize the impact of the noise in the height measurement, a high repetition rate is then used to improve the signal-to-noise ratio (SNR), especially when the ocean surface is rough, by the integration of several pulses to form a single ''tracker'' waveform that takes advantage of the available number of independent pulses at high wave heights, thus leading to a decrease in the SNR as SWH increases.

As recalled in Chelton et al. (2001), Walsh's (1982) paper has shown that the maximum pulse repetition rate for independent samples is a function of altimeter altitude and wavelength and is proportional to the square root of SWH, increasing from about 1000 pulses per second for 2-m SWH to about 3000 pulses per second for 10-m SWH. The PRFs are, respectively, 1020, 4500, 1200, and 1700 Hz, for GFO, TOPEX Ku band, TOPEX C band, and Poseidon (Quartly et al. 2001). Most successive altimeter pulses are therefore statistically independent for GFO, but fewer are for the T/P altimeters. As expected, above 2–3-m SWH, the TOPEX Ku-band actual 4500-Hz PRF does begin to provide range noise benefits in comparison with an approximately 1000-Hz PRF system such as GFO. So, the choice of different PRF for the different altimeters leads to the present results of different slopes of noise with SWH and to the ratio of Ku:C noise change with SWH for TOPEX.

To summarize and conclude, the assessment of the altimeter noise by high-pass filtering 1-Hz sea surface height time series can be applied to single-frequency altimeter data such as from GFO and the French altimeter Poseidon, as well as to dual-frequency altimeter data such as from TOPEX. As pointed out in an early analysis (Driscoll and Sailor 2001), this approach to estimating the altimeter noise provides results similar to those derived from the noise spectra computed from differenced repeating ground tracks and is also in agreement with the alternate operational TOPEX Ku-band range noise estimation method as presented in this paper.

This paper presents the first application of the high-pass-filtering method to multiple altimeters for determining the noise level in satellite altimeter data. This technique is found to be valuable because it allows the noise levels to be determined from individual tracks rather than from repeat tracks, facilitating time-dependent noise-level monitoring. The most obvious effect on the observed noise level is SWH, and, for all altimeters, the noise level increases linearly with increasing SWH. Other than the dependence on SWH, the noise level is very stable from cycle to cycle for GFO, TOPEX, and Poseidon. Thus, the high-pass-filtering technique will be useful for monitoring the performance of any altimeter as the satellite ages and for comparing the relative performance of different altimeters with respect to high-frequency noise.

As shown here, the effective number of independent radar return pulses directly affects altimeter range estimation precision. The new Poseidon-2 altimeters aboard the *Jason-1* satellite transmit at rates of 1800 and 300 Hz, for Ku and C band, respectively. Altimeters aboard *Envisat* operate at 1800 Hz at Ku band and 450 Hz at S band. These rates will thus set limits for both sensor's performance, as pointed out by Quartly et al. (2001).

Acknowledgments. The authors thank Ronald Brooks for his valuable comments, which helped us to produce a more comprehensive paper.

REFERENCES

Brammer, R. F., and R. V. Sailor, 1980: Preliminary estimates of the resolution capability of the Seasat radar altimeter. *Geophys. Res. Lett.,* **7,** 193–196.

Callahan, P. S., 1984: Ionospheric variations affecting altimeter measurement: A brief synopsis. *Mar. Geod.,* **8,** 249–263.

——, 1992: TOPEX/POSEIDON Project GDR user's handbook. Rep. D-8944, Jet Propulsion Laboratory, Pasadena, CA, 84 pp.

Chelton, D. B., J. C. Ries, B. J. Haines, L.-L. Fu, and P. S. Callahan, 2001: Satellite altimetry. *Satellite Altimetry and Earth Sciences: A handbook of Techniques and Applications,* L.-L. Fu and A. Cazenave, Eds., Academic Press, 463 pp.

Driscoll, M. L., and R. V. Sailor, 2001: *GFO* on-orbit altimeter noise assessment. NASA Tech. Memo. 2001-209984/Vol. 2 Rep. 21 pp. [Available online at http://gfo.wff.nasa.gov/docs.html.]

Fu, L.-L., E. J. Christensen, C. A. Yamarone Jr., M. Lefebvre, Y. Ménard, M. Dorrer, and P. Escudier, 1994: TOPEX/POSEIDON mission overview. *J. Geophys. Res.,* **99** (C12), 24 369–24 381.

Gaspar, P., F. Ogor, P. Y. Le Traon, and O.-Z. Zanife, 1994: Estimating the sea state bias of the TOPEX and POSEIDON altimeters from crossover differences. *J. Geophys. Res.,* **99** (C12), 24 981–24 994.

Imel, D. A., 1994: Evaluation of the TOPEX/POSEIDON dual-frequency ionosphere correction. *J. Geophys. Res.,* **99** (C12), 24 895–24 906.

LeSchack, A. R., and R. V. Sailor, 1988: A preliminary model for Geosat altimeter data errors. *Geophys. Res. Lett.,* **15,** 1203–1206.

Le Traon, P. Y., J. Stum, J. Dorandeu, and P. Gaspar, 1994: Global statistical analysis of TOPEX and Poseidon data. *J. Geophys. Res.,* **99** (C12), 24 619–24 631.

Marth, P. C., and Coauthors, 1993: Prelaunch performance of the NASA altimeter for the TOPEX/POSEIDON project. *IEEE Trans. Geosci. Remote Sens.,* **31,** 315–332.

Morris, C. S., and S. K. Gill, 1994: Evaluation of the TOPEX/POSEIDON altimeter system over the Great Lakes. *J. Geophys. Res.,* **99** (C12), 24 527–24 539.

Quartly, G. D., M. A. Srokosz, and A. C. McMillan, 2001: Analyzing altimeter artifacts: Statistical properties of ocean waveforms. *J. Atmos. Oceanic Technol.*, **18,** 2074–2091.

Sailor, R. V., 1993: Signal processing techniques. *Geoid and its Geophysical Interpretation*, P. Vanicek and N. Christou, Eds., CRC Press, 147–185.

——, and A. R. LeSchack, 1987: Preliminary determination of the Geosat radar altimeter noise spectrum. *Johns Hopkins APL Tech. Digest,* **8,** 182–183.

——, and M. L. Driscoll, 1992: Comparison of noise models and resolution capabilities for satellite radar altimeters. *Proc. Oceans 92 Conf.,* Newport, RI, IEEE, 249–253.

Stammer, D., and C. Wunsch, 1994: Preliminary assessment of the accuracy and precision of TOPEX/POSEIDON altimeter data with respect to the large-scale ocean circulation. *J. Geophys. Res.,* **99** (C12), 24 584–24 604.

Walsh, E. J., 1982: Pulse to pulse correlation in satellite radar altimeters. *Radio Sci.,* **17,** 786–800.

Zlotnicki, V., 1994: Correlated environmental corrections in TOPEX/POSEIDON, with a note on ionospheric accuracy. *J. Geophys. Res.,* **99** (C12), 24 907–24 914.